CERN SPSC 2006-040
SPSC-M-753
November 16, 2006

Status Report AD-4/ACE
Biological Effectiveness of Antiproton Annihilation

Michael H. Holzscheiter
for the AD-4 Collaboration.

Introduction

The main purpose of the AD-4/ACE experiment is to establish the feasibility of antiproton cancer therapy. We expect the biological effective dose deposited in the Bragg peak region for an identical effect in the entrance channel to be significantly higher for antiprotons than for protons and carbon ions. This is based on the observation that a small but biological significant portion of the annihilation energy is deposited by nuclear recoil ions in the vicinity of the annihilation point. As this portion of the energy is deposited by heavy ions the biological efficiency is further increased compared to a proton, enhancing the overall effect once more.

A first round of experiments conducted in 2003 and 2004 at CERN and at TRIUMF using proton and antiproton beams with approximately 50 MeV kinetic energy (which translates into a penetration in water of 22 mm) have shown a significant enhancement of the biological effective dose ratio (BEDR) between peak and plateau regions for beams of antiprotons compared to protons. The findings of these experiments have recently been published in Radiotherapy & Oncology (see attached).

After these initial findings we must now ask the question: “What clinical results could be expected from antiproton therapy based on these observation?” Currently, the only way to give a qualified answer to this question is through performing detailed planning studies for a number of specific cases, and then compare these results to the equivalent study using X-rays. protons, and antiprotons. For this type of study a precise knowledge of both physical dose and biological effects of the antiproton beam is required.

2006 Run Period

The 2006 run period concentrated on issues that will positively impact these questions. The measurement separated in too distinct groups, dosimetry and biological effects, and were performed at a beam energy of 125 MeV. The main reason for requesting this higher energy was to achieve a deeper penetration into the target. At 50 MeV (or 22 mm waterequivalent depth in the target) the effective penetration into the biological target (accounting for additional material intercepting the beam before the target like beam monitors and entrance windows for the experiment) was only 10 mm. The deeper penetration depth allowed a clear separation of the entrance channel and the proton-like behaviour of the antiproton beam in this region from the biological impact due to the annihilation events near the Bragg peak. Furthermore, the natural straggling in the target led to a width of the pristine Bragg peak that was compatible with the biological analysis method. This allowed us to generate a data set which can more easily

be compared to theoretical model calculations. In addition, the deeper penetration allowed a more precise study of the effects of inflight annihilation and enabled us to generate a spread-out Bragg peak with a width of 10 mm. Latter has been consistently requested by oncologists since a clinically spread-out Bragg peak will alter the Peak to Plateau ratio and especially increase the effects in the entrance channel.

The physical dose distributions predicted by Monte Carlo calculations using the code FLUKA are shown for both the pristine peak and the spread-out Bragg peak in figure 1.

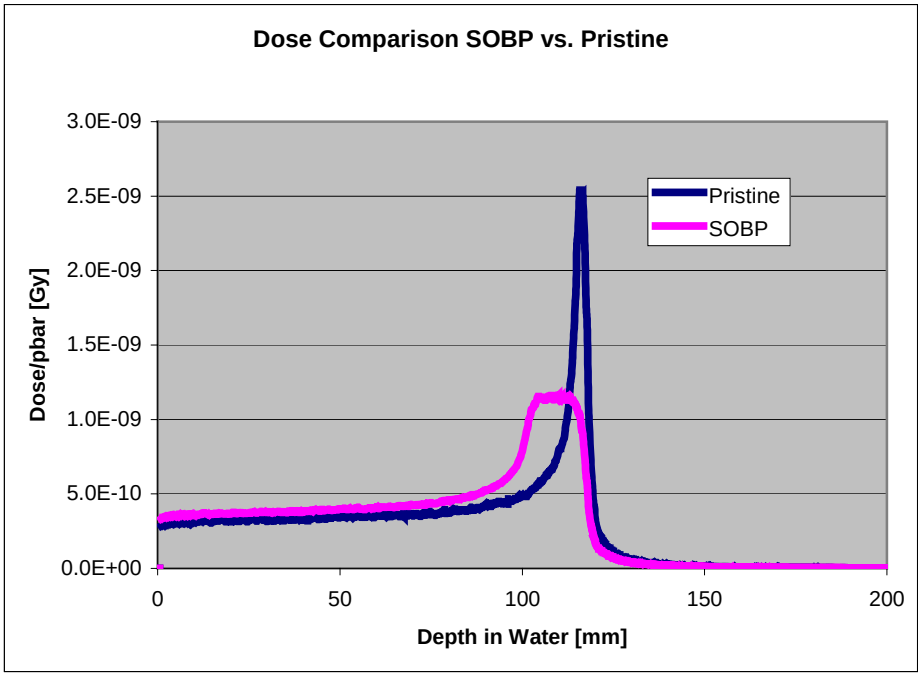

Figure 1: Physical dose distribution for pristine and spread-out Bragg peaks calculated by FLUKA for a 125 MeV antiproton beam

In addition to the standard dosimetry measurements using Alanine tablets and GAF chromic film we used for the first time a set of ionization chambers provided by the DKFZ in Heidelberg. One of the chambers was mounted in front of the water phantom to be used as a calibration tool and the second one could be moved axially with the help of a precision caliper. We performed an extensive study across the parameter space for the operating voltage of these chambers with the intention to look for saturation effects due to the high instantaneous dose rate presented by the short duration of the AD beam pulses. This analysis is not yet completed but from the raw data we immediately could see that these instruments provided the most stable (relative) measurement of the incoming beam intensity shot to shot. We are currently working on extracting an absolute calibration for the plateau region which would then allow us to use these chambers as an absolute dosimetry tool for future studies. In the mean time we can compare the relative dose profile of these measurements with the FLUKA calculations and find excellent agreement (Figure 2).

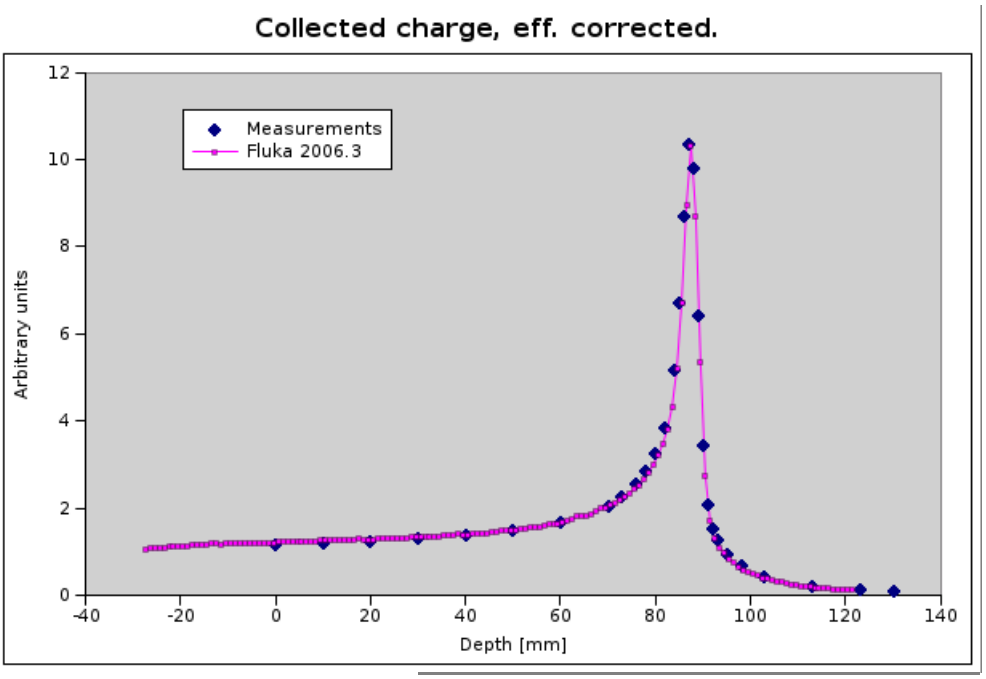

Figure 2.: Comparison between FLUKA prediction and measurements using an ionization chamber for a pristine peak. Peak height was normalized as an absolute calibration of the chamber has not yet been performed.

For the biological measurements we used the exact same methods as in 2003 and 2004 with the only difference being the length of the gel tubes necessary to accommodate the 100 mm effective depth of the Bragg peak in the target. Cell preparation and the analysis of the clonogenic survival measurements were performed at the laboratory of Brad Wouters at the University of Maastricht. An early analysis has shown that the measurement produced reasonable results but a quantitative analysis has not been performed yet due to the lack of time since the end of the run at CERN. In addition to the standard clonogenic survival measurements we also performed a set of irradiations with the spread-out Bragg peak using a human cancer cell line (FaDu) that was used by our collaborators from the Department of Clinical Oncology at the University Hospital in Aarhus to study genetic expressions following irradiations of cells with a variety of radiation types using micro array analysis. The interest in using an antiproton spread-out Bragg peak lies in the fact that the mixture of high LET and low LET radiation significantly varies across the depth of the Bragg peak from the proximal side to the distal edge. Slices of gel material through out the Bragg peak as well as from a location in the plateau have been prepared and fixated and the final analysis will be performed when the experimental knowledge of the exact location of the Bragg peak has been determined from the clonogenic survival studies (the cost of the analysis per slice in the micro array assay is substantial and we want to only analysis the absolute minimum of samples using this method).

CERN SPSC 2006-040
SPSC-M-753
November 16, 2006

Summary

We have made significant progress in developing the Monte Carlo capability for the biological effect of antiprotons and have now several codes available for benchmarking purposes. These include SHIELD-HIT, FLUKA, and MCNPX. We plan to use our experimental data and results from the benchmarking calculations obtained from these different MC codes as input to the local effect model developed at GSI to produce the first planning studies of antiproton therapy. In addition we are discussing with the GEANT User's Group the necessary changes to use the latest version of GEANT together with the biological modules recently implemented for estimates of physical dose and biological effectiveness of antiproton irradiation

The data collected in this run period will assist us in fine tuning our predictive capabilities and will guide us in future experiments. Future work will concentrate on the following topics:

1. Finalizing our data set for physical and biological dose in the antiproton beam.
2. Quantitative measurements of biological effects in the immediate surrounding of the beam (distal to the Bragg peak and radial penumbra).
3. Stochastic effect due to high energy, minimum ionizing annihilation products in the far field (several centimeters away from the direct beam).

A detailed description of future work can only be given after the complete analysis of the latest run has been completed.

Radiotherapy and Oncology xx (2006) xxx–xxx
www.thegreenjournal.com

Original article

The biological effectiveness of antiproton irradiation

Michael H. Holzscheiter[a], Niels Bassler[b,h,i], Nzhde Agazaryan[c], Gerd Beyer[d], Ewart Blackmore[e], John J. DeMarco[c], Michael Doser[f], Ralph E. Durand[g], Oliver Hartley[d], Keisuke S. Iwamoto[c], Helge V. Knudsen[b], Rolf Landua[f], Carl Maggiore[a], William H. McBride[c], Søren Pape Møller[b], Jørgen Petersen[h,i], Lloyd D. Skarsgard[g], James B. Smathers[c], Timothy D. Solberg[c], Ulrik I. Uggerhøj[b], Sanja Vranjes[k], H. Rodney Withers[c], Michelle Wong[g], Bradly G. Wouters[j,*]

[a]*Pbar Labs, LLC, Santa Fe, NM, USA,* [b]*Deparment of Physics & Astronomy and ISA, University of Aarhus, Aarhus, Denmark,* [c]*David Geffen School of Medicine at UCLA, Los Angeles, CA, USA,* [d]*Centre Medicale Universitaire, Geneva, Switzerland,* [e]*TRIUMF, Vancouver, BC, Canada,* [f]*CERN, PH Department, Geneva, Switzerland,* [g]*British Columbia Cancer Research Centre, Vancouver, BC, Canada,* [h]*Department of Medical Physics, and* [i]*Department of Experimental Clinical Oncology, Aarhus University Hospital, Aarhus, Denmark,* [j]*Vinca Institute of Nuclear Sciences, Belgrade, Serbia and Montenegro,* [k]*Department of Radiation Oncology (Maastro Lab), GROW Research Institute, University of Maastricht, The Netherlands*

Abstract

***Background and purpose*: Antiprotons travel through tissue in a manner similar to that for protons until they reach the end of their range where they annihilate and deposit additional energy. This makes them potentially interesting for radiotherapy. The aim of this study was to conduct the first ever measurements of the biological effectiveness of antiprotons.**

***Materials and methods*: V79 cells were suspended in a semi-solid matrix and irradiated with 46.7 MeV antiprotons, 48 MeV protons, or ^{60}Co γ-rays. Clonogenic survival was determined as a function of depth along the particle beams. Dose and particle fluence response relationships were constructed from data in the plateau and Bragg peak regions of the beams and used to assess the biological effectiveness.**

***Results*: Due to uncertainties in antiproton dosimetry we defined a new term, called the biologically effective dose ratio (BEDR), which compares the response in a minimally spread out Bragg peak (SOBP) to that in the plateau as a function of particle fluence. This value was $\sim$3.75 times larger for antiprotons than for protons. This increase arises due to the increased dose deposited in the Bragg peak by annihilation and because this dose has a higher relative biological effectiveness (RBE).**

***Conclusion*: We have produced the first measurements of the biological consequences of antiproton irradiation. These data substantiate theoretical predictions of the biological effects of antiproton annihilation within the Bragg peak, and suggest antiprotons warrant further investigation.**

Keywords: Antiproton; RBE; Particle irradiation; High LET

For conventional photon irradiation, the maximum dose that can be delivered to a tumor is limited by the tolerance of irradiated adjacent normal tissues. Several technological improvements in radiation delivery, including intensity-modulated radiotherapy (IMRT), have made it possible to confine the high-dose region to almost any target volume of interest and thus reduce the dose to adjacent tissues [1–3]. However, even with these techniques, normal tissue tolerances can prevent delivery of a dose sufficient to achieve tumor cure. IMRT also results in a larger total body exposure and thus an increased risk of secondary cancers [4]. For many types of tumors, this has led to unacceptably low tumor control probability (TCP) and to high levels of morbidity. An alternative approach involves the use of protons and other heavier ions [5–8]. For these charged particles, both the amount and rate of energy deposition increase dramatically as the particle nears the end of its range. This results in a large enhancement in absorbed dose at a precise depth in tissue (the Bragg peak) compared with the dose deposited at the entrance to the body (the pla-

0167-8140/$ - see front matter doi:10.1016/j.radonc.2006.09.012

Please cite this article in press as: Holzscheiter MH et al., The biological effectiveness of antiproton irradiation, Radiother Oncol (2006), doi:10.1016/j.radonc.2006.09.012

teau). For treatment purposes, the position of the Bragg peak needs to be spread out to cover the tumor volume and the production of such a spread-out Bragg peak (SOBP) results in a build up of plateau dose and hence a reduction in the ratio of dose in the SOBP relative to the plateau. However, in contrast to photons, the dose in the SOBP that covers the tumor volume remains larger than that in the normal tissue entrance region. High linear energy transfer (LET) particles such as carbon ions also produce a much higher ionization density in the Bragg peak region and consequently an increase in the relative biological effectiveness (RBE) of the dose deposited in the tumor [9–11]. This provides a potential further therapeutic advantage, especially for tumors that have a large hypoxic fraction or for those that are resistant to conventional radiation [12]. Furthermore, since very little dose is deposited distal to the Bragg peak, charged particles are ideally suited for treatments of tumors close to radiosensitive regions. These favorable physical and biological characteristics have led to recent developments of proton and heavy ion cancer therapy centers worldwide.

Conversion of the mass of a proton–antiproton pair during annihilation constitutes the highest density energy source currently available. This has led to a number of proposals for practical applications of antiprotons, including radiotherapy, which is feasible with current antiproton production technology [13]. Like other charged particles, antiprotons deposit most of their kinetic energy near the end of their path in the Bragg peak. In addition, as an antiproton comes to rest it annihilates, depositing additional energy in the form of particles that may have a significantly enhanced biological effectiveness [14]. The majority of the total annihilation energy of 1.88 GeV is carried away by high-energy pions, neutrons and γ-rays. We have estimated (unpublished data) that the dose deposition from these particles is of a similar magnitude to that reported for a passively degraded proton beam [4]. However, at the Bragg peak it has been estimated that antiprotons deposit an additional 30 MeV within a few millimeters of the annihilation vertex [15]. The only experimental data relevant to the application of antiprotons for biological purposes were produced by Sullivan [16], who measured the relative physical dose deposition in the plateau and the Bragg peak regions for antiprotons at the low energy antiproton ring (LEAR) at CERN. He found that although the additional local dose deposited is small compared to the total annihilation energy, it does represent an approximate doubling of the physical dose deposited per particle in the Bragg peak compared to protons. Furthermore, the RBE of this additional dose is likely to be significantly higher than that for protons because it is due partly to recoiling heavy fragments produced in the annihilation event with short range and high LET. The remainder of the annihilation energy that is carried away,outside of the body, could potentially be used for real-time imaging of the dose distribution.

To date there has been no attempt to assess the biological effects of antiprotons. This stimulated us to initiate an experiment, AD-4/ACE [17,18], running at the antiproton decelerator (AD) at CERN, to measure the biological effects of antiproton irradiation and compare it to the results achievable with protons.

Materials and methods

Beam characteristics

The AD at CERN delivered a 200–500 ns beam pulse containing approximately 3×10^7 antiprotons every 85 s. For our experiment the extraction energy was 46.7 MeV. In order to spread the Bragg peak we used a ridge filter consisting of a plastic sheet machined with a matrix of pixels $\sim$1 mm^2 in area. Three pixel thicknesses (1, 1.8 and 2.6 mm) were used at a ratio of 41:31:28 to create a SOBP as smooth as possible over a distance of slightly more than 2.5 mm. The degrader was placed 25 cm upstream of the target so that the lateral straggling together with the free drift in air would remove any radial dose inhomogeneity from the degrader in the samples. A schematic of the set-up is shown in Fig. 1.

For proton irradiation, we utilized the treatment facility located at TRIUMF, details of which have been previously published [19]. The energy was reduced to 48 MeV with a range shifter to closely match the energy of the antiproton beam. The proton Bragg peak was also spread out over an area slightly larger than 2.5 mm using a two-step rotating wedge filter in order to create a dose profile which matched that of the antiproton as close as possible.

For ^{60}Co irradiation, a Theratron unit at the Vancouver Cancer Centre was used as described previously [19].

Dosimetry

Due to the pulsed nature of the antiproton beam it was not possible to use currently available dosimetry equipment to measure absorbed dose. The large number of antiprotons delivered in such a short period of time leads to saturation, non-linearity and unreliability of conventional equipment such as ionization chambers. Thus, in order to estimate the absorbed dose and the relative depth dose profile we carried out a Monte Carlo simulation based on measurements of antiproton fluence using the MCNPX code [20]. Antiproton fluence was monitored using two independent methods. After the ridge filter the antiproton beam passed through a current monitor (Bergoz[1] BCM/ICT) capable of integrating a pulse with rise times as short as a few picoseconds without significant loss. The voltage was then held level for about 400 μs for read-out. The signal processor used two integrating windows to correct for baseline noise and therefore achieved high accuracy for low beam current. In our set-up the sensitivity was 1 mV/6.3×10^5 antiprotons, resulting in a typical read-out of 50 mV per pulse. The noise was less than 5 mV, allowing a fluence measurement to within 10%. We also received a signature from the accelerator on the number of antiprotons having left the ring upon ejection, which was typically within 20% of the ICT measurement indicating a high-transfer efficiency to our experiment.

In order to estimate the dose with Monte Carlo methods, it was also necessary to determine the radial-beam profile, and thus the fraction of antiprotons that enter the biological sample. We monitored the integrated beam profile using GAF chromic film, which darkens in a linear way with dose. Because the sensitivity is low, it was necessary to integrate

[1] BERGOZ Instrumentation, Espace Allondon Ouest, 06130 Saint Genis Pouilly, France.

Please cite this article in press as: Holzscheiter MH et al., The biological effectiveness of antiproton irradiation, Radiother Oncol (2006), doi:10.1016/j.radonc.2006.09.012

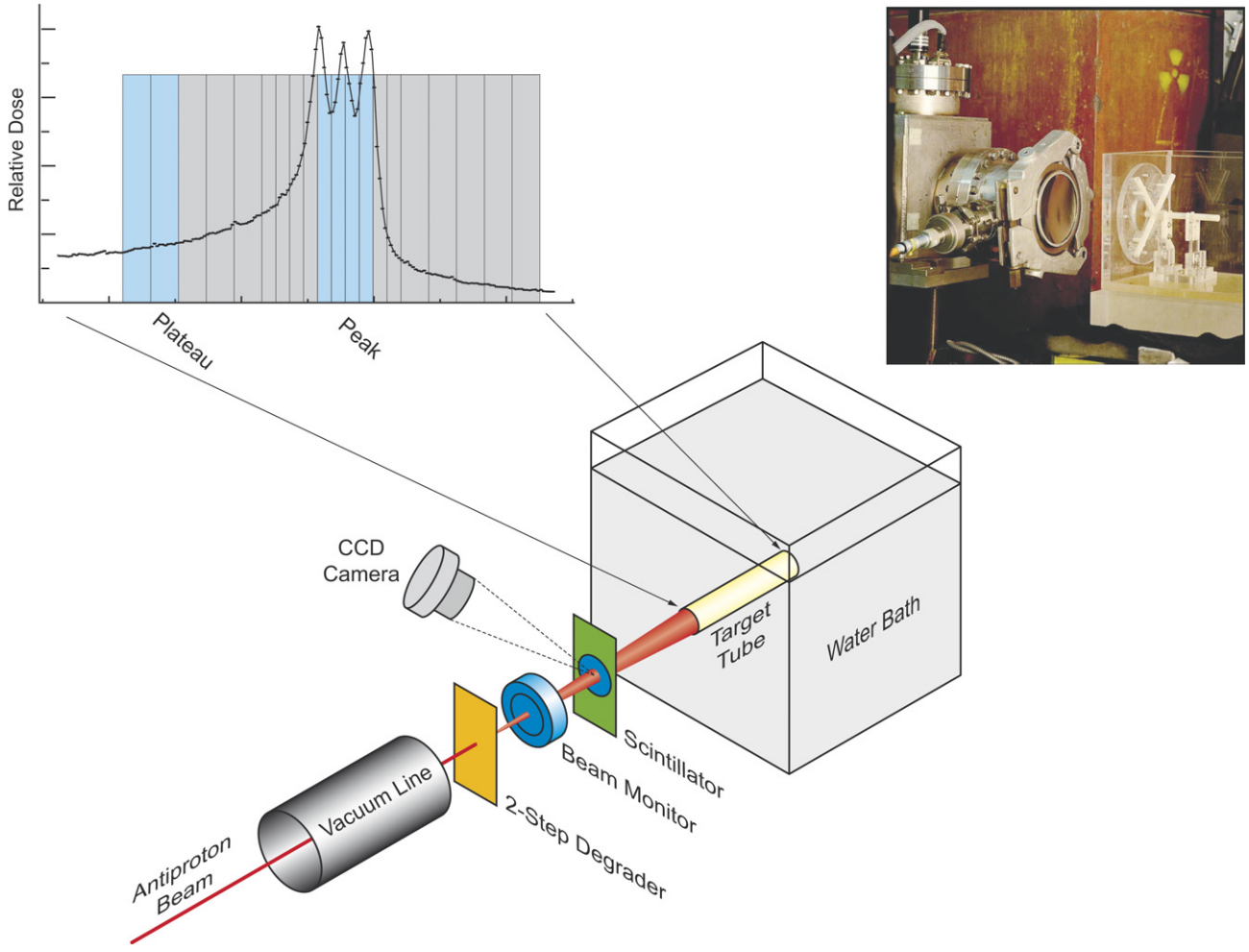

Fig. 1. Schematic set-up of the antiproton experiment. The antiproton beam leaves the accelerator vacuum through a thin titanium window, passes through a two-step ridge filter, a beam current monitor and a scintillator before entering a plexiglass tank containing a glycol/water mixture and the biological sample (see photo inset upper right). Also shown are the antiproton dose profile and the slicing protocol for extracting cell survival data after the irradiation.

over 1–2 h. To monitor individual pulses, we developed a system consisting of a thin sheet of BC-400 scintillator material intercepting the beam without affecting energy or straggling significantly. This material was placed near the entrance to the phantom and viewed by a sensitive CCD camera.[2] To reduce noise, the camera was synchronized with the arrival of the pulse, and the signal was sufficient to obtain the beam profile and to determine the centroid and diameter of a single shot from the AD. This system also allowed us to adjust the beam position in sub-millimeter increments. Only the central part of the Gaussian-shaped beam was used to ensure a radial variation of less than 5%.

For protons, the delivered dose was measured by a calibrated transmission chamber and relative depth–dose measurements were carried out with a parallel plate ionization chamber.

[2] APOGEE Instruments Inc., KX1E Digital Imaging System, comprising a TE cooled camera head with Grade 2 Kodak KAF-0401E CCD.

Measurement of clonogenic survival

We chose to use V79-WNRE cells in these studies because this cell line has been used previously to quantify the biological characteristics of other particle beams [19]. We employed a modified form of the sliced-gel technique of Skarsgard and co-workers [19,21] coupled with the cell sorter survival assay, details of which are published elsewhere [19,22]. Briefly, cells were cultured in MEM supplemented with 10% fetal bovine serum and maintained in exponential growth. Cells were harvested with trypsin, and re-suspended at 2×10^6 cells/ml in MEM containing 20% FBS and 12% gelatin (gel/medium). At 37 °C, this was a viscous fluid and for proton and antiproton irradiations, was poured into ABS (acrylonitrile butadiene styrene) plastic tubes of 0.6 cm inside diameter and 18 cm length, with a piston located so as to accommodate a 6-cm deep cylinder of gel/medium. For ^{60}Co irradiation, 0.5–1 ml samples of the cell/gel suspension were deposited into 5 ml plastic test tubes. After solidification at 4 °C the tubes were sealed and stored on ice.

For irradiation, sample tubes were placed with their axis collinear with the beam axis, in a circulating, refrigerated bath containing a 19.3% glycerol/water solution. The densi-

Please cite this article in press as: Holzscheiter MH et al., The biological effectiveness of antiproton irradiation, Radiother Oncol (2006), doi:10.1016/j.radonc.2006.09.012

ties of materials encountered by the beam (ABS tube, gel/medium, glycerol/water) were carefully chosen to produce identical stopping powers throughout the entire phantom. The cells were maintained at 2 °C throughout the irradiation procedure and were kept on ice prior and subsequent to irradiation. This maintained the spatial organization of the cells, and also avoided dose-rate effects that would have otherwise confounded measurements (individual sample antiproton exposures were as long as 16 h). Only the central part of the antiproton beam was used to irradiate the cell sample tube, thus assuring an intensity variation across the sample of less than 5%. After irradiation, the gel was extruded from the tube and cut into slices of 0.5 or 1 mm thickness. These slices were melted in warm culture medium and a cell sorter was then used to sort an accurately known number of cells from each sample. Two to three sorts from each slice were plated into individual 100-mm Petri dishes with 14 ml of culture media and allowed to form colonies (defined as >50 cells) for 6–7 days. A sufficient number of cells was plated to produce ~400–500 colonies per dish. Three slices upstream of the SOBP which received zero primary dose were used to measure the plating efficiency (PE).

For comparison purposes we also measured the clonogenic survival response of V79 cells in the gelatin-matrix to ^{60}Co irradiation. This served as both a reference to measure the RBE for protons and also allowed us to control for any minor variations in the radiosensitivity of the cells between experiments. For antiproton experiments, samples were prepared at CERN and irradiated in Vancouver after transport. For proton experiments, ^{60}Co samples were irradiated at times similar to the proton samples.

Determination of RBE and BEDR

The goal of our experiments was to obtain an estimate of the biological effect of antiprotons. Conventionally, this property would be the RBE, which is equal to the ratio of absorbed dose between the conventional and test irradiation producing the same level of survival. For proton irradiation it was possible to determine RBE because we have a reliable measure of dose. RBE was calculated as the ratio of ^{60}Co to proton doses which resulted in the same level of cell survival. Dose values were determined from linear quadratic (LQ) fits to the survival data.

It was not possible to calculate a similar RBE for antiprotons because we did not have a reliable measure of the absorbed dose. Thus, it was necessary to design comparative experiments in such a way that measurement of absolute dose was not required. To do this we compared survival responses obtained in the SOBP with those obtained in the plateau following delivery of a known number of particles (fluence). Because the dose in the plateau and the SOBP are directly proportional to the fluence, it is possible to compare the responses without knowing the conversion factor from fluence to dose. We defined a new term called the biologically effective dose ratio (BEDR), equal to the ratio of plateau to SOBP fluences required to produce a defined level of survival.

$$\mathrm{BEDR} = \frac{\mathrm{Fluence}_{\mathrm{plateau}}}{\mathrm{Fluence}_{\mathrm{peak}}},$$

where $\mathrm{Fluence}_{\mathrm{plateau}}$ and $\mathrm{Fluence}_{\mathrm{peak}}$ are the different fluences that produce the same level of cell survival. It can be shown that BEDR is numerically equal to

$$\mathrm{BEDR} = F\frac{\mathrm{RBE}_{\mathrm{peak}}}{\mathrm{RBE}_{\mathrm{plateau}}},$$

where F is the ratio of the physical dose deposited in the SOBP to that deposited in the plateau.

Results

Physical dose

The axial physical dose profiles of the proton and antiproton beams are shown in Fig. 2. For protons, this figure represents the measured relative dose as a function of depth in water and for antiprotons it is a Monte Carlo estimate based on conversion from particle fluence measurements. The modulation of dose in the Bragg peak results from the use of the discrete two-step degrader with a step size comparable to the width of the pristine Bragg peak for this energy. As expected, the peak to plateau dose ratio is much larger for antiprotons than for protons. Defining a point 7 mm upstream as the plateau yields a measured dose ratio of 2.0 for protons and an estimated 4.0 for antiprotons. The positions and widths of gel slices used to measure clonogenic survival in different regions of the beam are also shown.

Because samples were irradiated over a 24-h period at CERN and then transported to Vancouver, the cells were maintained in gel at cold temperatures for 42–54 h. The PE measured from each sample tube, as well as the PE from several unirradiated controls allowed us to monitor the consequences of this exposure (see Fig. 3a). Although, there was a small trend towards increased toxicity with time (a drop in PE from ~0.7–0.6), the PE remained high throughout the experiment and comparable to that measured previously[19]. Fig. 3b shows the ^{60}Co survival curves determined during both the proton experiment at TRIUMF and the antiproton experiment in CERN. The similarity of these two responses also indicates that the long exposure to gel did not significantly affect radiosensitivity.

Survival data

Fig. 4a and b show the clonogenic survival determined from individual gel slices plotted as a function of depth throughout the proton and antiproton beams. The depth in gel has been converted to its stopping-power equivalent depth in water. All material in front of the gel (the gel cap, tank window, and other materials) has also been converted to water equivalent depth and included so that the plots represent the total particle range.

For the proton experiment, cell survival was determined from 20 individual slices as a function of depth in each of eight sample tubes receiving a different dose to the SOBP. The dose range to the SOBP was 1–14Gy and resulted in survival measurements over 1 log in both the peak and plateau regions. The survival responses are in good agreement with expectations from the measured dose distributions shown in the upper panel. The steep dose gradient beyond the edge

Please cite this article in press as: Holzscheiter MH et al., The biological effectiveness of antiproton irradiation, Radiother Oncol (2006), doi:10.1016/j.radonc.2006.09.012

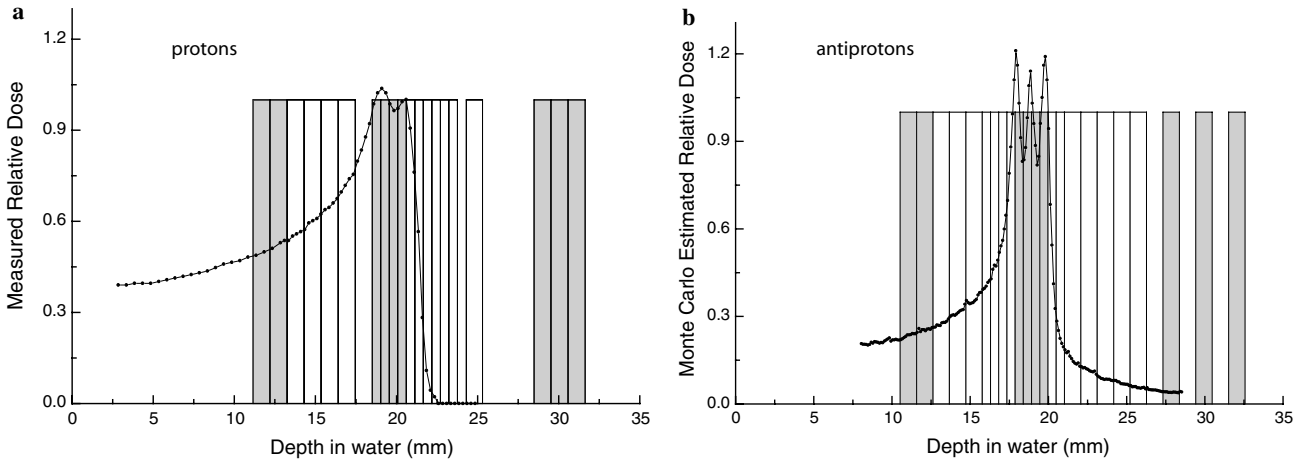

Fig. 2. Physical dose profiles and slicing protocol. The measured physical dose along the axis of the range-modulated proton beam at TRIUMF (a) and the Monte Carlo estimated physical dose along the axis of the range-modulated antiproton beam at CERN (b) are shown as a function of depth in water. The SOBP is approximately 2.5 mm in width. Also plotted are the positions and widths of gel slices from which clonogenic survival was determined. Four positions in the peak (2 mm total width), and two positions 7 mm upstream from the peak center (2 mm total width) were used to determine average values for the SOBP and plateau, respectively (shaded areas). Three slices beyond the Bragg peak were used to determine plating efficiency.

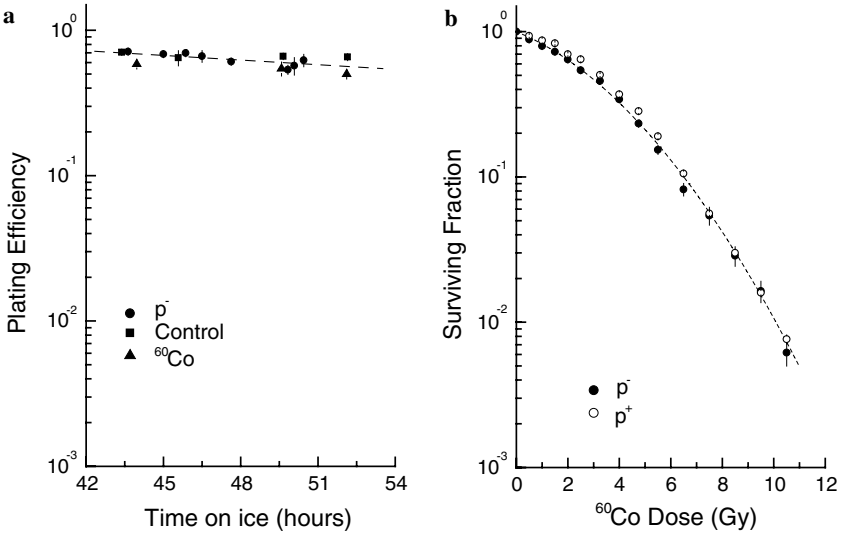

Fig. 3. Plating efficiency and radiosensitivity during extended exposure to gelatin. The plating efficiency of V79-WNRE cells as a function of time at 0 °C in the gelatin matrix from samples used during one of the antiproton experiments (a). Plating efficiency was determined from individual sample tubes that received antiproton irradiation (p^-), or from untreated control tubes (control). Plating efficiencies of the ^{60}Co control samples are also shown (^{60}Co). The clonogenic survival of V79-WNRE cells is shown as a function of ^{60}Co dose (b). These ^{60}Co-response curves were derived from samples prepared during the antiproton experiment at CERN (p^-) and during the proton experiment at TRIUMF (p^+).

of the SOBP allowed us to verify the positioning of the sample tube to less than 0.5 mm.

Fig. 4b shows similar data obtained following irradiation with antiprotons. Because it was not possible to measure absolute dose, we used the estimates based on measured antiproton fluence and Monte Carlo models. Survival data were determined at 23 positions in depth for six individual sample tubes irradiated with estimated peak doses between 1 and 25Gy. These data demonstrate a much higher difference between the peak and plateau regions. Interestingly, the non-uniform dose in the SOBP predicted by Monte Carlo analysis is reflected in these measurements.

RBE and BEDR

In Fig. 5a, we have plotted the survival as a function of absorbed dose for both proton and ^{60}Co irradiation. The proton dose responses were constructed from the data shown in Fig. 4a. The survival in the peak region was calculated from the average of the four 0.5 mm slices located within the SOBP and the survival in the plateau was calculated as the

Please cite this article in press as: Holzscheiter MH et al., The biological effectiveness of antiproton irradiation, Radiother Oncol (2006), doi:10.1016/j.radonc.2006.09.012

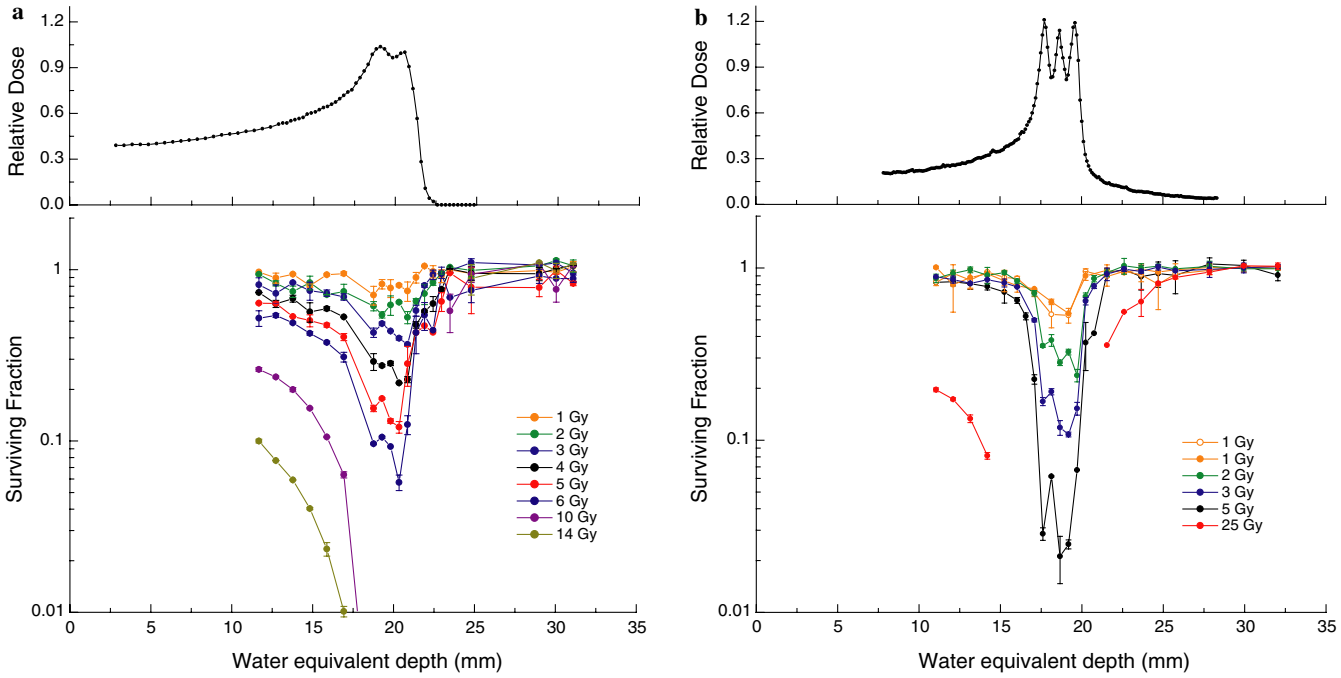

Fig. 4. Clonogenic survival response to antiprotons and protons. The clonogenic survival of V79-WNRE cells is plotted as a function of water equivalent depth along the axis of the proton beam (a) and antiproton beam (b). Survival was measured in 20 individual gel slices after proton irradiation and in 23 slices after antiproton irradiation in individual tubes irradiated with a range of peak doses. Each line represents a single tube irradiated with the measured proton (a) or estimated antiproton (b) dose to the SOBP. For reference, the physical dose profiles are shown in the upper frames.

average of two 1 mm slices located 7 mm upstream (see also Fig. 2a). The relative dose in the plateau at this point was 51% of that in the peak. The resulting dose response in the plateau is indistinguishable from that for ^{60}Co irradiation, and thus the RBE in this region is 1. The radiation sensitivity of cells irradiated in the SOBP is significantly higher. We used the LQ model to fit the ^{60}Co and proton SOBP responses and then calculated the RBE at different levels of survival (Fig. 5a). The RBE_{20} (RBE at a surviving fraction of 20%) for the proton SOBP is equal to 1.2, in good agreement with previous measurements with this system [19].

In Fig. 5b and c, we have replotted the plateau and SOBP survival as a function of particle fluence rather than absorbed dose. In this manner, the response in the SOBP appears far more sensitive than in the plateau (compare proton data in Fig. 5a and b). This arises because the absorbed dose per particle in the SOBP is higher (for protons ~2-fold) and additionally because the RBE in the SOPB is higher. These fluence based survival responses were then fit using the LQ equation, and the resulting parameters used to calculate the BEDR. This value is equal to the ratio of fluences in the plateau and the peak that give the same level of cell survival. At 20% survival the BEDR for protons is 2.4.

The survival responses in the SOBP and plateau regions of the antiproton beam are shown as a function of fluence in Fig. 5c. These plateau data were calculated as the average survival from two 1 mm slices located 7 mm upstream of the SOBP, and the SOBP response is taken from the average of the four 0.5 mm slices located within the SOBP region. Data extracted from the data set shown in Fig. 4b are labeled as Exp1. Also shown in Fig. 5c, are data obtained from a smaller experiment carried out 3 months prior (Exp 2). The BEDR for antiprotons determined from LQ fits to these data is shown in the lower frame of Fig. 5c. At 20% survival the antiproton BEDR is equal to 9.0, or about 3.75 times higher than for protons.

Antiproton RBE

Although, we could not directly measure antiproton RBE, it is possible to make an estimate of this value based on the measurements presented so far. The ratio of BEDR for antiprotons to protons is equal to:

$$\frac{BEDR(p^-)}{\mathrm{BEDR}(p^+)} = \frac{F(p^-)}{F(p^+)} \cdot \frac{\mathrm{RBE}(p^-)_{\mathrm{peak}}/\mathrm{RBE}(p^-)_{\mathrm{plateau}}}{\mathrm{RBE}(p^+)_{\mathrm{peak}}/\mathrm{RBE}(p^+)_{\mathrm{plateau}}}.$$

This can be rearranged to determine the RBE for antiprotons in the SOBP:

$$\mathrm{RBE}(p^-)_{\mathrm{peak}} = \frac{\mathrm{BEDR}(p^-)}{\mathrm{BEDR}(p^+)} \cdot \frac{F(p^+)}{F(p^-)} \cdot \frac{\mathrm{RBE}(p^-)_{\mathrm{plateau}}}{\mathrm{RBE}(p^+)_{\mathrm{plateau}}} \cdot \mathrm{RBE}(p^+)_{\mathrm{peak}}.$$

The only value in this equation that has not been estimated or measured is the antiproton RBE in the plateau. However, this value is equivalent to the proton plateau RBE provided that in-fight annihilation dose is insignificant. We estimated the consequence of in-flight annihilation by finding an accurate universal fit to all measured annihilation cross sections known to us, from which we calculated the effect in our specific case [23]. Using our knowledge of the stopping power of antiprotons we then calculated the number of remaining antiprotons, and the electronic energy deposited along the beam path (Fig. 6a). Here, we have ignored elastic

Please cite this article in press as: Holzscheiter MH et al., The biological effectiveness of antiproton irradiation, Radiother Oncol (2006), doi:10.1016/j.radonc.2006.09.012

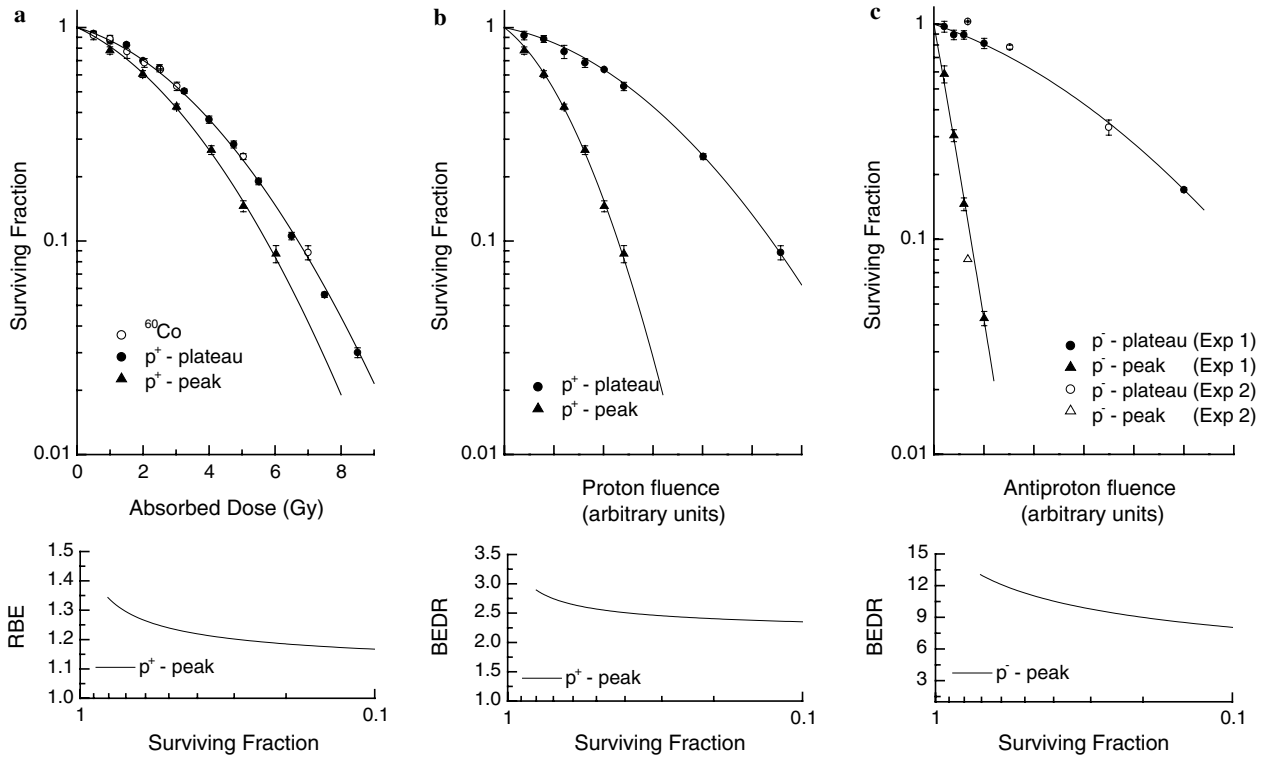

Fig. 5. Determination of RBE and BEDR. The average survival of cells within the SOBP and plateau region of the proton beam are plotted as a function of absorbed dose (a, upper frame). These data were fit with the LQ model, and the resulting parameters used to calculate the RBE as a function of surviving fraction (a, lower frame). In (b), the same proton data from (a) are plotted as a function of proton fluence (upper frame) and fits to these data were used to calculate the BEDR (lower frame). In (c, upper frame), the average survival of cells within the SOBP and plateau region of the antiproton beam are plotted as a function of antiproton fluence. Fits to these data were used to calculate the antiproton BEDR (c, lower frame). In the text, BEDR and RBE values are quoted at a survival of 20%. At this level of survival, the BEDR for antiprotons is approximately 3.75-fold higher than for protons due to the increased annihilation dose in the SOBP and its higher RBE.

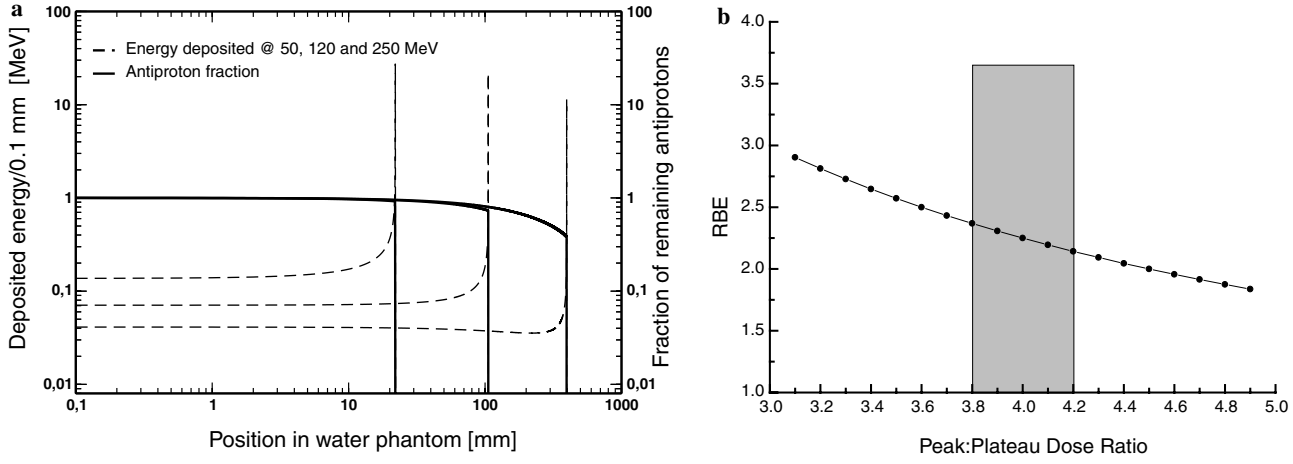

Fig. 6. Estimation of RBE in the antiproton SOBP. The amount of deposited energy along the tracks of 50, 120 and 250 MeV antiprotons passing through water (dashed lines) (a). Also shown in this plot are the remaining fractions of antiprotons for each of these energies (solid curves). In (b) the RBE in the antiproton SOBP has been estimated for different values of the peak to plateau dose ratio. The product of the RBE and this ratio is equal to the measured BEDR. The shaded area represents the best estimate for the dose ratio.

scattering as well as transport of secondary particles and assumed that each annihilation deposits 30 MeV of energy locally. The loss of antiprotons with an initial energy of 50 MeV due to in-flight annihilation is very small (8%) and even for higher energies up to a depth of 40 cm, a distinct Bragg peak remains.

Please cite this article in press as: Holzscheiter MH et al., The biological effectiveness of antiproton irradiation, Radiother Oncol (2006), doi:10.1016/j.radonc.2006.09.012

Thus, if we assume equivalent plateau RBE values, the antiproton RBE in the SOBP becomes the following:

$$\mathrm{RBE}(p^-)_{\mathrm{peak}} = \frac{\mathrm{BEDR}(p^-)}{\mathrm{BEDR}(p^+)} \cdot \frac{F(p^+)}{F(p^-)} \cdot \mathrm{RBE}(p^+)_{\mathrm{peak}}.$$

The only value that has not been directly measured in this equation is the dose ratio (F) for antiprotons. However, if we use the Monte Carlo estimate of 4.0 for this value as depicted in Fig. 2b, the antiproton RBE in the SOBP is equal to 2.25. Because we are not completely certain of the Monte Carlo dose estimates we have also plotted in Fig. 6b the relationship between F and the peak RBE for antiprotons that is required to produce the measured BEDR_{20} value of 9.0.

Discussion

The biological effectiveness of antiprotons

The data presented here are the first measurements to date of the biological consequences of antiproton irradiation. The nature of the antiproton beam made it impossible to determine standard dose–response curves that could be compared with low-LET radiation to determine the RBE. We thus defined the BEDR, a new term that is based on comparing the responses in the peak and plateau regions as a function of particle fluence. This value is biologically meaningful, because it represents a direct measurement of the gain in 'biologically equivalent dose' deposited in the Bragg peak region compared to that in the plateau. Since the dose deposition in the plateau is essentially identical for proton and antiproton beams of similar energy, a comparison of the BEDR of protons with that of antiprotons provides a direct measure of the additional biological consequences of annihilation events at the Bragg peak.

At 20% survival the BEDR_{20} for antiprotons was equal to 9.0 and for protons it was 2.4- or 3.75-fold lower. The BEDR for antiprotons increased because of two factors: (i) the increase in the ratio of dose deposited in the SOBP relative to the plateau due to the annihilation dose and (ii) the increase in the RBE of the extra annihilation dose. For protons, the RBE in the SOBP was 1.2 and the peak to plateau dose ratio was 2.0. The product of these two values gives the BEDR value of 2.4. For antiprotons our best estimate of the peak to plateau dose ratio is 4.0-, or 2-fold higher than that for protons. This results in an estimate of the antiproton SOBP RBE of approximately 2.25 provided that the RBE in the plateau region is similar to that for protons. Our estimation of in-flight annihilation dose indicates that this effect is indeed small, suggesting that this assumption is valid. Given the fact that the annihilation dose in the peak accounts for only an estimated 50% of the total dose in this area, an average RBE of 2.25 in this region implies that the RBE for the dose contributed by annihilation must be very high.

Comparison to carbon ions

It would be interesting to compare our measurements with other high LET particles, such as carbon ions. Blakely et al. [9] measured cell survival in pristine peaks of 400 MeV/u carbon ions using the Berkeley Bevalac. Range straggling in this high-energy beam yielded a Bragg peak of stopping width similar to our modulated proton and antiproton beams (~3 mm at 80% of maximum). We estimated the BEDR for this carbon ion beam to be 7.9, using a definition for the plateau point reflecting the situation encountered at CERN (7 mm upstream). However, the much greater range of the carbon ions adds uncertainty to this estimate. Because the gradient on the proximal side of the Bragg peak changes drastically with penetration depth, it is difficult to make a proper choice for the plateau definition. Weyrather et al. [10,11] have also reported RBE values for a range of carbon ion energies. Using SRIM [24] we calculated a dose profile for a pristine carbon beam with a range equivalent to our set-up at CERN and estimated the maximum BEDR from the Weyrather data to be 8.5 (after correcting for the loss of primary ions due to fragmentation). This result is for an unmodulated pristine Bragg peak. Spreading the Bragg peak to a width similar to that in our experiment significantly lowers the peak to plateau-dose ratio and hence the BEDR. We estimated this would reduce the BEDR to ~5. High uncertainties in this analysis have prompted us to begin a comparison measurement for carbon ions using a set-up equivalent to that at CERN.

Another important consideration in the comparison of antiproton irradiation with other high-LET particles is the value of the RBE upstream of the Bragg peak. As discussed above, the RBE for antiprotons in the plateau region is not expected to be different from that for protons. Because the contribution of in-flight annihilation is small, the biological dose deposited outside of the Bragg peak per particle is essentially the same as that for a proton. This would have a significant clinical advantage over other high LET particles such as carbon ions, which have RBE values significantly greater than 1 in the plateau region of the depth-dose curve. As a consequence, it is not possible to use the clinical experience with low-LET radiations to estimate normal tissue tolerances without making an assumption for the RBE. Because high-LET particles often have RBE values that are energy, dose and cell type specific, one must use caution in the application of these particles in the clinic. For antiprotons, because the annihilation dose (high-LET component) would be confined to the tumor, it would be possible to treat using established normal tissue dose tolerances.

Peripheral damage

An important aspect for any new irradiation concerns the biological consequences of dose that may be deposited outside of the primary beam. Initial attempts to assess peripheral damage caused by antiproton annihilation suggest it is quite small. Even for the highest dose used in our experiments, which resulted in a surviving fraction of 20% in the plateau, we observed ~55% survival at only 2 mm distal to the Bragg peak (see Fig. 3). Furthermore, we also made preliminary measurements of clonogenic survival in sample tubes placed perpendicular to the beam at the Bragg peak. These data also indicate that the peripheral dose is small (data not shown). Further experimental studies in the peripheral regions using beams with peaks spread according

Please cite this article in press as: Holzscheiter MH et al., The biological effectiveness of antiproton irradiation, Radiother Oncol (2006), doi:10.1016/j.radonc.2006.09.012

to clinically relevant criteria will be required to fully quantify these effects.

Conclusion

In conclusion, our experiment has produced the first direct measurements of the biological consequences of antiproton irradiation. It substantiates theoretical predictions and earlier speculations on the consequences of antiproton annihilation within the Bragg peak [15,25]. For the beams compared in our study, the BEDR for antiprotons was 3.75-fold larger than the BEDR for protons, which represents a substantial increase in effective dose within the SOBP. In a treatment situation, a higher energy beam with a larger SOBP would be required to treat tumors of a reasonable size. As a result, the peak to plateau dose ratio for either a proton or antiproton beam would be significantly reduced, and the comparison would yield a value below the value observed here. However, antiprotons would retain a significant biological dose advantage due to the contribution of both the annihilation dose and its high estimated RBE. In this regard, it is important to note that there are a number of treatment situations in which increases in tumor dose as small as 10–20% can produce significant improvements in outcome.

Future research has to show if the advantages of antiprotons in terms of (a) higher physical dose in the Bragg peak, (b) the increased RBE confined to the Bragg peak and (c) the real-time imaging capability will warrant their serious consideration as an alternative modality for tumor irradiation. At that time it will be necessary to analyze both the technical and financial problems posed by the antiproton production process. While the actual treatment center will be similar to a standard proton center, the production of antiprotons requires accelerating protons to 20–30 GeV. With current technology this requires a synchrotron of about 100–200 m in diameter. Production, capture, storage and delivery of antiprotons will require a number of additional accelerator rings. CERN currently produces a modest amount of antiprotons that suffice for limited biological studies. GSI is planning the construction of a high energy addition to their existing facility which will make available antiprotons useful for irradiation at greater depths at intensities sufficient for standard irradiation times and realistic tumor volumes [26]. This facility could theoretically be used to further evaluate and develop antiproton treatment clinically.

Acknowledgements

The Danish Cancer Society supported the project with a grant. Some of us (N.B., H.V.K., S.P.M., U.I.U.) have been supported by the ICE center under the Danish Science Research Council.

* **Corresponding author. Bradly G. Wouters**, Department of Radiation Oncology, Maastricht Radiation Oncology (Maastro) Lab, GROW Research Institute, USN50/23 University of Maastricht, P.O. Box 616, 6200MD Maastricht, The Netherlands. *E-mail address:* brad.wouters@maastro.unimaas.nl

Received 27 June 2006; received in revised form 6 September 2006; accepted 13 September 2006

References

[1] Lof J, Lind BK, Brahme A. An adaptive control algorithm for optimization of intensity modulated radiotherapy considering uncertainties in beam profiles, patient set-up and internal organ motion. Phys Med Biol 1998;43:1605–28.
[2] Group ICW. Intensity-modulated radiotherapy: current status and issues of interest. Int J Radiat Oncol Biol Phys 2001;51:880–914.
[3] Williams PC. IMRT: delivery techniques and quality assurance. Br J Radiol 2003;76:766–76.
[4] Hall EJ. Intensity-modulated radiation therapy, protons, and the risk of second cancers. Int J Radiat Oncol Biol Phys 2006;65:1–7.
[5] Levin WP, Kooy H, Loeffler JS, DeLaney TF. Proton beam therapy. Br J Cancer 2005;93:849–54.
[6] Suit H, Goldberg S, Niemierko A, et al. Proton beams to replace photon beams in radical dose treatments. Acta Oncol 2003;42:800–8.
[7] Schulz-Ertner D, Nikoghosyan A, Thilmann C, et al. Carbon ion radiotherapy for chordomas and low-grade chondrosarcomas of the skull base. Results in 67 patients. Strahlenther Onkol 2003;179:598–605.
[8] Mazeron JJ, Noel G, Feuvret L, Calugaru V, Racadot S. Clinical complementarities between proton and carbon therapies. Radiother Oncol 2004;73:S50–2.
[9] Blakely EA, Tobias CA, Yang TC, Smith KC, Lyman JT. Inactivation of human kidney cells by high-energy monoenergetic heavy-ion beams. Radiat Res 1979;80:122–60.
[10] Weyrather WK, Kraft G. RBE of carbon ions: experimental data and the strategy of RBE calculation for treatment planning. Radiother Oncol 2004;73:S161–9.
[11] Weyrather WK, Ritter S, Scholz M, Kraft G. RBE for carbon track-segment irradiation in cell lines of differing repair capacity. Int J Radiat Biol 1999;75:1357–64.
[12] Svensson H, Ringborg U, Naslund I, Brahme A. Development of light ion therapy at the Karolinska Hospital and Institute. Radiother Oncol 2004;73:S206–10.
[13] Slater JM. Considerations in identifying optimal particles for radiation medicine. Technol Cancer Res Treat 2006;5:73–9.
[14] Kraft G, Scholz M, Bechthold U. Tumor therapy and track structure. Radiat Environ Biophys 1999;38:229–37.
[15] Gray L, Kalogeropoulos TE. Possible biomedical applications of antiproton beams: focused radiation transfer. Radiat Res 1984;97:246–52.
[16] Sullivan AH. A measurement of the local energy deposition by antiprotons coming to rest in tissue-like material. Phys Med Biol 1985;30:1297–303.
[17] Maggiore C, Agazaryan N, Bassler N, Blackmore E, Beyer G, DeMarco JJ, et al. Biological effectiveness of antiproton annihilation. Nucl Instrum Meth B 2004;214:181–5.
[18] Holzscheiter MH, Agazaryan N, Bassler N, Beyer G, DeMarco JJ, Doser M, et al. Biological effectiveness of antiproton annihilation. Nucl Instrum Meth B 2004;221:210–4.
[19] Wouters BG, Lam GK, Oelfke U, Gardey K, Durand RE, Skarsgard LD. Measurements of relative biological effectiveness of the 70 MeV proton beam at TRIUMF using Chinese hamster V79 cells and the high-precision cell sorter assay. Radiat Res 1996;146:159–70.
[20] Waters LS, Hendricks JS, Hughes HG, McKinney GW, Snow EC. Medical Applications of the MCNPX Code. American Nuclear Society, 12th Biennial Radiation Protection and Shielding Division Topical Meeting, Santa Fe, NM, 8-89448-667-5, ANS Order No. 700293 April 14–18, 2002.

[21] Skarsgard LD, Palcic B, Douglas BG, Lam GK. Radiobiology of pions at TRIUMF. Int J Radiat Oncol Biol Phys 1982;8:2127–32.
[22] Durand RE. Use of a cell sorter for assays of cell clonogenicity. Cancer Res 1986;46:2775–8.
[23] Bassler N, Holzscheiter M, Knudsen H, Collaboration AD-4/ACE. Cancer therapy with antiprotons. LEAP, American Institute of Physics, CP796, AIP Conference Proceedings 2005. p. 423–30.
[24] Ziegler JF, Biersack JP, Littmar U. The Stopping and Range of Ions in Solids. New York: Pergamon Press; 2003.
[25] Kalogeropoulos TE, Muratore R. Antiprotons for imaging and therapy. Nucl Instrum Meth B 1989;B40–41:1322–5.
[26] Gross K, Eschke J. Facility for antiproton and ion research (FAIR). Nucl Phys News 2006;16:5–8.

Please cite this article in press as: Holzscheiter MH et al., The biological effectiveness of antiproton irradiation, Radiother Oncol (2006), doi:10.1016/j.radonc.2006.09.012